# Increased Potential of Bone Formation With Intravenous Injection of Parathyroid Hormone-minicircle DNA Vector

**Jang-Woon Kim**
Catholic University of Korea College of Medicine: Catholic University of Korea School of Medicine
**Narae Park**
Catholic University of Korea College of Medicine: Catholic University of Korea School of Medicine
**Jaewoo Kang**
Catholic University of Korea College of Medicine: Catholic University of Korea School of Medicine
**Yena Kim**
Catholic University of Korea College of Medicine: Catholic University of Korea School of Medicine
**Hyerin Jung**
Catholic University of Korea College of Medicine: Catholic University of Korea School of Medicine
**Ji Hyeon Ju** ( juji@catholic.ac.kr )
Catholic iPSC Research Center, College of Medicine, The Catholic University of Korea,

**Research article**

**Keywords:** Osteoporosis, Ovariectomized mice, Minicircle DNA vector, Parathyroid hormone-related protein, Trabecular bone structure

**Posted Date:** October 9th, 2020

**DOI:** https://doi.org/10.21203/rs.3.rs-88110/v1

# Abstract

**Background:** Osteoporosis is usually treated with long-term usage of anti-osteoporotic agents. However, poor drug compliance and emerging side effects sometimes are limitations for the treatment of osteoporosis. Parathyroid hormone-related protein (PTHrP) is needed for normal bone formation and remodeling. We attempted a new method using minicircle vectors (mc) encoding PTHrP analogs.

**Methods:** We generated mc encoding the infusion of PTHrP 1-34 with 107-139 (mc 1-34+107-139). Ovariectomized (OVX) model was induced in 12-week-old C57BL/6 female mice. mc 1-34+107-139 was administered three times weekly via intravenous injections.

**Results:** mc 1-34+107-139 significantly increased bone formation compared with the OVX group and decreased the bone resorption. PTHrP mc DNA vector was effective in increasing the quality of trabecular bone structure.

**Conclusions:** These results provide experimental evidence for the therapeutic potential of minicircle DNA vectors in OVX model. This study is a first attempted proof-of-concept gene therapy using minicircle vectors for the treatment of osteoporosis.


# Background

Osteoporosis is one of the bone diseases in which loss of bone strength leads to fragility fractures. Osteoporosis is accompanied by a decrease in the trabecular bone number and thickness of trabecular bone.[1, 2] There are 3 categories of osteoporosis: 1) primary (estrogen deficiency and age), 2) secondary (endocrine and metabolic, drugs and genetic disorders), and 3) idiopathic (fractures in young adults of unknown cause).[3] Estrogen deficiency at menopause impairs the normal bone metabolism by increasing osteoclastic resorption without a corresponding increase in osteoblastic activity. This process involving bone remodeling is described as uncoupling. Thus, the trabecular bones are not only reduced and thinned, but also the trabecular bone plate changes to a rod-like structure, which increases the risk of osteoporosis fractures.[2] Currently, postmenopausal osteoporosis treatments are predominantly drug-based, and inhibit bone resorption and bone anabolism. The anti-resorptive agents demonstrated an increase in bone mineral density (BMD) and decreased fracture risk in clinical trials. Recent studies reported that the anti-resorptive agents induce negative effects via excessive suppression of physiological bone turn over their long term use. The mechanism of anabolic agents increase bone formation via bone metabolism in osteoblasts. [4, 5] Parathyroid hormone (PTH) analogs and PTH-related peptide (PTHrP) analogs are approved by the United States Food and Drug Administration (FDA) as anabolic agents for the treatment of osteoporosis in the United States.[6] PTHrP domains include the PTH-like N-terminal PTHrP peptide and the C-terminal PTHrP peptide. PTHrP-null mice represent a form of skeletal haploinsufficiency characterized by decreased bone volume. [7] Daily administration of PTHrP 1–36 and PTHrP 107–139 to ovariectomized (OVX) animals resulted in similar osteogenic effects. In addition, PTHrP 107–139 dramatically inhibited the osteoclast proliferation gene marker expression (DKK

1 and Sost) and decreased the bone resorption markers in OVX mice.[8] Another study reported that the recombinant hPTHrP 1–84 was more effective than hPTHrP 1–34 in enhancing renal calcium reabsorption and stimulating bone formation in OVX mice.[9] However, the anti-resorptive and bone anabolic agents showed side-effects and poor long-term efficacy for postmenopausal osteoporosis treatment.[10] Therefore, new drugs or gene therapies are needed for postmenopausal osteoporosis. Studies reported that gene therapy for osteoporosis using adenoviral vector-containing osteoprotegerin (OPG) and various cytokines such as interleukin (IL-1) and tumor necrosis factor (TNF) resulted in increased bone volume and reduced osteoclast surface in the proximal tibial metaphysis.[11–14] However, gene therapy for osteoporosis requires a nontoxic delivery vector and adequate preclinical safety. [11] In our previous studies, we confirmed the minicircle (mc) vector system as an alternative option given the high cost of the development and production of biologics in vitro and in vivo. The mc vectors show higher gene transfer efficiency via chemical methods compared with plasmid-based (non-viral) physical methods. In our previous study, we confirmed that mc vector injection into collagen-induced arthritic mice resulted in drug synthesis. [15–18] However, the mc vector system is not currently studied in animal models of osteoporosis. We investigated the possibility of therapeutic application of mc PTHrP 1–34 + 107–139 gene therapy provide experimental evidence for therapeutic application in the OVX model of osteoporosis.

## Materials And Methods

# PTHrP Sequence and Minicircle (mc) Vector production

We utilized the sequence of PTHrP 1–34 and 107–139 described by Toshiyuki et.al.[19] To construct the therapeutic minicircle, PTHrP 1–34 + 107–139 (282 bp) sequences were sub-cloned into the parental plasmid pMC. The CMV-MCS-EF1-GFP-SV40-Poly A was purchased from SBI (System Biosciences, # MN501A-1). The mc Mock and mcPTHrP 1–34 + 107–139 were synthesized as described by Park and Kay et.al. [15–16] The mc DNA vector was isolated using the Nucelobond Xtra Midi kit (Macherey-Nagel, # 740410.100). We confirmed the successful generation of sequences containing mc PTHrP 1–34 + 107–139 with Bam HI and Xbal via gel imaging.

# Hek 293t Cell Culture And Minicircle Vector Transfection

Human embryonic kidney (HEK293T) cells were cultured in Dulbecco's Modified Eagle Medium (DMEM; Thermo Fisher Scientific, #11965-092) supplemented with 7.5% fetal bovine serum (FBS), 100 U/mL penicillin and 100 µg/mL streptomycin (Thermo Fisher Scientific,#15240096). HEK293T cells were transfected with the minicircle vectors (Mock, PTHrP1-34 + 107–139) using a Lipofectamine 2000 reagent (Thermo Fisher Scientific, #11668019) following the manufacturer's instructions. The expression of GFP and PTHrP antibodies (Novusbio, #3H1-5G8) in the cells was assessed via immunofluorescence staining under microscopy. The gene expression of the inserted sequence of PTHrP 1–34 + 107–139 was confirmed by RT-PCR in the cell lysate.

# Hmscs Cell Culture And Minicircle Vector Transfection

Bone marrow-derived human mesenchymal stem cells (MSCs) were purchased from The Catholic Institute of Cell Therapy, South Korea. MSCs were maintained in DMEM (Thermo Fisher Scientific, #11965-092) supplemented with 20% FBS, 100 U/mL penicillin and 100 µg/mL streptomycin (Thermo Fisher Scientific, #15240096). At passage 5, MSCs ($1 \times 10^6$ cells) were transfected with minicircle vectors for microporation using the Neon transfection system (Thermo Fisher Scientific, #MPK5000S). Several conditions were tested for the microporation of minicircle vector transfection. Microporation at 1400 pulse voltage, 20 pulse width, and 2 pulse no was used for the transfection of MSCs at passage 5. The immunophenotypes of the non-transfected MSCs and mc PTHrP 1–34 + 107–139 MSCs at passage 5 were determined using CD 34, CD45, CD73 and 105 (BD Biosciences) using flow cytometric analysis.

# Animal Experiment And Group Allocation

C57BL/6 female mice (Orient bio Inc, Korea) aged 12 weeks with a mass range of 17 to 23 g were ovariectomized to induce postmenopausal osteoporosis. Mice were randomized to the following groups: sham (health control) group (n = 3), OVX (disease control) group (n = 6), mc PTHrP 1–34 + 107–139 (n = 5), MSCs (n = 4), and eMSCs (mc PTHrP 1–34 + 107–139 MSCs, n = 6). Animal experiment procedures were reviewed and approved by the Animal Studies Committee of the School of Medicine, The Catholic University of Korea (IACUC approval No.CUMC-2017-0250-03).

# Delivery And Detection Of Mc Pthrp 1–34 + 107–139 In Vivo

The plasmid mc PTHrP 1–34 + 107–139 DNA vector was delivered hydrodynamically using intravenous injection into the tail vein. Mice were injected with 40 µg of 1.8 mL PBS three times each week for 3 weeks at 4 weeks post-OVX. The eMSCs ($1 \times 10^6$ cells) were resuspended in 150 µL of PBS. Cells were injected twice at 4 and 6 weeks, post-OVX via intraperitoneal injection. mc PTHrP 1–34 + 107–139 was delivered to C57BL6 female mice for 12 weeks, into organs such as spleen, kidney and liver at 3, 7, 15 and 37 days after the injection. After co-staining GFP-positive cells with PTHrP (Novusbio) antibody, the homogenizes tissues were extracted with TRIzol solution. RT-PCR was carried out using inserted PTHrP 1–34 + 107–139 sequence primers based on gel images.

# Micro Ct Analysis

At 10 weeks post-OVX, the distal femurs were imaged at a scanning voxel size of 13.85 µm with a high-resolution microtomographic system (Sky Scan 1173). Using the SkyScan of Nrecon (ver. 1.7.0.4) reconstruction program, the bone microarchitectural parameters in the trabecular bone regions were calculated to determine the trabecular-specific surface area (BS/BV) based on the trabecular bone

microarchitecture for trabecular thickness (Tb.Th), trabecular bone pattern factor (Tb.Pf), and structure model index (SMI).

# Measurement Of Bone Turnover Markers In Serum

Blood samples were collected at 10 weeks post-OVX. To evaluate bone remodeling markers in the serum, the bone formation marker N-terminal propeptide of type 1 procollagen (PINP) and the bone resorption marker C-terminal telopeptide of type 1 collagen (CTX-1) were measured using enzyme immune-assays (EIA). PINP and CTX-1 concentrations were evaluated via Rat/Mouse PINP EIA (Immunodiagnostic Systems, # AC-33F1) and RatLaps™ EIA (Immunodiagnostic Systems,# AC-06F1).

# Statistics Analysis

All results were expressed as mean ± SEM in the figures and the legends. The results were analyzed using Kruskal-Wallis using SPSS program (IBM Corporation). Inter-group comparisons were done using Mann-Whitney analysis. A *P* value of less than 0.05 was considered statistically significant.

## Results

# Generation of mc PTHrP 1–34 + 107–139 Vector in vitro

We designed and performed following the mc PTHrP1-34 + 107–139 as shown in (Fig. 1A). Successful generation of mc PTHrP was confirmed by arabinose treatment. By splicing the plasmid with Bam HI and X-bal, we confirmed that the cloned PTHrP 1–34 + 107–139 sequences were inserted accurately (Fig. 1B). We confirmed that the generated mc PTHrP 1–34 + 107–139 vector was expressed using green fluorescent protein (GFP) in HEK293T cells at 48 h post-transfection (Fig. 1C). Upon co-staining with PTHrP marker and GFP positive cells, the co-expression of PTHrP was observed in mcPTHrP 1–34 + 107–139 at 48 hours post-transfection (Fig. 1D). The PTHrP 1–34 + 107–139 gene sequences in the mc PTHrP 1–34 + 107–139 only showed that the PTHrP 1–34 + 107–139 gene expression in HEK293T cells persisted at 48 hours post-transfection (Fig. 1E).

In vivo **detection of mc PTHrP 1–34 + 107–139**

To investigate the duration of long minicircle-affected cells *in vivo*, mc PTHrP 1–34 + 107–139 was delivered to C57BL6 female mice, and their spleens, kidneys and livers were obtained at 3, 7, 15 and 37 days after the injection. They were analyzed by immunofluorescence staining with PTHrP antibody (Fig. 2A and C), and the gene expression was determined using the inserted PTHrP 1–34 + 107–139 sequence primers based on gel images (Fig. 2E and G). In the spleen tissue, the PTHrP antibody and 1–34 + 107–139 gene expression was detected at 15 d and 37 days, GFP positive cells with co-localization with PTHrP antibody markers (green and red) under high-power (x1000) magnification was confirmed

using a LSM 510 Meta confocal microscope respectively, after the injection. Expression of PTHrP started to increase on day 15 in spleen tissue (Fig. 2A, D and E). The levels of PTHrP antibody and 1–34 + 107–139 gene expression were increased on day 15, and decreased on day 37 after the injection into the kidney tissue (Fig. 2B and F). GFP positive cells with co-localization with PTHrP antibody markers (green and red) under high-power (x1000) magnification was confirmed (Fig. 2D). The PTHrP antibody and 1–34 + 107–139 gene expression increased rapidly to the level seen on day 7 and to the levels seen on days 15 and 37 in the liver tissue (Fig. 2C and G). GFP positive cells with co-localization with PTHrP antibody markers (green and red) under high-power magnification was confirmed (Fig. 2D).

### The mc PTHrP 1–34 + 107–139 increased the quality of trabecular bone and the expression of bone formation, and decreased the serum bone resorption in OVX mice

To investigate the in vivo effects of mc PTHrP 1–34 + 107–139, we injected OVX mice with mc PTHrP 1–34 + 107–139 three times weekly intravenously (Fig. 3A). At 10 weeks post-OVX, assessments of bone microarchitecture in the distal femurs (0.5-2 mm) were conducted using micro CT (Fig. 3B) and reconstruction programs (Fig. 3C-F). The bone quantitative parameters of bone fraction (BV/TV) and trabecular bone numbers in the mc PTHrP 1–34 + 107–139 did not increase the bone mass compared with the mice subjected to OVX(disease control), at 10 weeks post-OVX (data not shown). However, the Tb.Th was significantly higher in the mc PTHrP 1–34 + 107–139 than in the OVX mice (Fig. 3C). The Tb.Pf was significantly lower in the mc PTHrP 1–34 + 107–139 than in the OVX (Fig. 3D). The BS/BV, especially the trabecular bone density was significantly decreased in the mice exposed to mc PTHrP 1–34 + 107–139 than the OVX mice (Fig. 3E). The structural model index of trabecular bone was significantly lower in the mc PTHrP 1–34 + 107–139 than in the OVX mice (Fig. 3F). The levels of bone turn over markers PINP (bone formation) and CTX-1 (bone resorption) in the serum at 10 weeks post-OVX, suggested that the PINP expression in the mc PTHrP 1–34 + 107–139 was associated with a significantly higher bone formation than the OVX mice (Fig. 3G). The CTX-1 expression in the mc PTHrP 1–34 + 107–139 showed a greater decrease in bone resorption compared with the OVX (Fig. 3H).

### Therapeutic application of mc PTHrP 1–34 + 107–139 synthesizing MSCs in OVX mice model

We generated engineered MSCs (eMSCs) named as mc PTHrP 1–34 + 107–139 MSCs using a novel strategy in OVX mouse models. We verified that mc PTHrP 1–34 + 107–139 was functional in HEK 293T cells, and therefore, this vector was used to transfect MSCs via microporation using the Neon transfection system. To investigate the effect of eMSCs *in vivo*, we intraperitoneally injected OVX mice with MSCs and eMSCs twice (4 and 6 weeks) weekly (Fig. 4A). We confirmed that the eMSCs expressed GFP at 48 h after transfection under inverted fluorescence microscope (Fig. 4B) and used FACS analysis to confirm that eMSCs did not disrupt the MSCs phenotype. The expression of negative markers (CD45 and CD29) and positive markers (CD73 and CD105) of MSCs in eMSCs was similar to MSCs at passage 5 (Fig. 4C). We confirmed that eMSCs were successfully generated and maintained the phenotype of MSCs after transfection. At 10 weeks post-OVX, the bone microarchitecture of the distal femurs (0.5-2 mm) was assessed using micro CT (Fig. 4D) and the reconstruction method (Fig. 4E and F). The bone quantitative

parameter of bone fraction (BV/TV) and trabecular bone numbers in the mc PTHrP 1–34 + 107–139 MSCs did not increase the bone mass compared with the OVX mice at 10 weeks post-OVX (data not shown). The Tb.Th was higher in the eMSCs than in the OVX and MSCs (Fig. 4E). The structural model index of trabecular bone was lower in the eMSCs than in the OVX and MSCs. However, no significant differences were detected compared with the OVX and MSCs (Fig. 4F). The PINP expression in the eMSCs showed a significantly higher bone formation than the OVX and MSCs (Fig. 4G). The CTX-1expression in the eMSCs showed a greater decrease in bone resorption compared with than the OVX and MSCs (Fig. 4H).

# Discussion

Parathyroid hormone (PTH)-related peptide (PTHrP) is expressed by cells in the early osteoblastic lineage, suggesting a role for PTHrP in bone cell regulation. We generated a vector enclosing the nucleotide sequence of PTHrP 1–34 (involved in bone formation) combined with 107–139 (for ostoclast inhibition) based on the plasmid minicircle structure and to develop a new method using mc vectors encoding biological drugs in OVX mice. Our previous results reported that mc express genes longer than in other previously published methods without integrating into the host genome. [16–18]In our experiments, the expression of the inserted PTHrP 1–34 + 107–139 gene sequence was increased in the spleen and kidney of mice at 15 days after injection with mc PTHrP 1–34 + 107–139. Interestingly, the expression of the PTHrP antibody and 1–34 + 107–139 gene was higher on day 7 and slightly lower than the gene expression on days 15 and 37 in the liver, which can be explained by the initial migration of mc PTHrP 1–34 + 107–139 and subsequent PTHrP expression.

Ovariectomy decreased parameters such as BV/TV, Tb.N, and Tb.Th, but increased Tb.Sp and SMI in mice over several weeks.[20] To our knowledge, after minicircle injection, mc PTHrP 1–34 + 107–139 did not increase BV/TV and Tb.N in OVX mice. However, mc PTHrP 1–34 + 107–139 significantly increased Tb.Th and decreased BS/BV, Tb.Pf and SMI parameters compared with mice exposed to OVX mice, at 10 weeks. The SMI and BS/BV values are influenced by the morphological changes in the trabeculae, and transformation from plate-like to rod-like structure. Furthermore, the critical stress intensity factor values were correlated with the microarchitecture of the osteoporotic cancellous tissue.[21, 22]

Bone turnover occurs via bone resorption and formation of CTX-1 and PINP, which are the markers of bone resorption and formation, respectively. [23] Our present study suggests that the bone turnover markers in serum are elevated during bone formation as the PINP expression was significantly higher in the mc PTHrP 1–34 + 107–139 group than in the OVX mice at 10 weeks post-OVX. In contrast, the serum level of bone resorption marker CTX-1 in the mc PTHrP 1–34 + 107–139 was significantly lower compared with the OVX mice at 10 weeks. The amount of bone resorption equals that of bone formation subsequently in every bone remodeling unit (remodeling balance). However, after menopause, in the bone remodeling unit, the amount of new bone formation is reduced compared with the bone newly resorbed in the same remodeling cycle (remodeling imbalance). Increased concentrations of bone turnover markers may be associated with increased bone loss and fracture risk in postmenopausal women. [20]

We previously confirmed a potential alternative for the delivery of biologics using mc TNFR2MSCs and cell-based therapy in CIA mice.[16] To our knowledge, this is the first study to confirm the therapeutic application of mc-transfected MSCs (mc PTHrP 1–34 + 107–139 MSCs) in OVX mice. Based on our results, we conclude that the injected mc PTHrP 1–34 + 107–139 restored the remodeling balance in OVX mice.

# Conclusion

mc PTHrP 1–34 + 107–139 efficiently enhanced the quality of trabecular bone structure and increased new bone formation; it also decreased the levels of newly resorbed bone in the bone remodeling cycle of OVX mice. The mc PTHrP 1–34 + 107–139 MSCs increased new bone formation and decreased bone resorption in the bone remodeling cycle in the serum compared with mice exposed to MSCs and OVX mice. Although this strategy is at the proof-of-concept stage, it represents a potential alternative delivery of biologics using mc PTHrP 1–34 + 107–139 and eMSCs (mc PTHrP 1–34 + 107–139 MSCs), gene- and cell-based therapy in OVX mouse models of osteoporosis.

# Abbreviations

**PTHrP**
Parathyroid hormone-related protein, **mc**:minicircle DNA vectors, **OVX**:Ovariectomized, **BMD**:bone mineral density, **PTH**:Parathyroid hormone, **FDA**:Food and Drug Administration, **OPG**:osteoprotegerin, **IL-1**:interleukin-1, **TNF**:tumor necrosis factor, **HEK293T**; Human embryonic kidney cells, **FBS**:fetal bovine serum, **MSCs**:mesenchymal stem cells, **eMSCs**:engineered mesenchymal stem cells, **BS/BV**:Bone surface area /Bone volume, **BV/TV**:Bone volume/total volume, **Tb.N**:Trabecular Number, **Tb.Th**:Trabecular thickness, **Tb.Pf**:Trabecular bone pattern factor, **Tb.Sp**:Trabecular spacing, SMI:Structure model index, **PINP**:N-terminal propeptide of type 1 procollagen, **CTX-1**:C-terminal telopeptide of type 1 collagen.

# Declarations

### Ethics approval and consent to participate

Animal experiment procedures were reviewed and approved by the Animal Studies Committee of the School of Medicine, The Catholic University of Korea (IACUC approval No.CUMC-2017-0250-03).

### Consent for publication

Not applicable.

### Availability of data and materials

All data generated and analyzed during this study are included in this article. Materials used in this study are available from the corresponding author on reasonable request.

### Competing interests

There are no financial conflicts of interest to disclosure. The authors declare no competing interests.


### Funding

This work was supported by a grant of the Korea Healthcare Technology R&D project, Ministry for Health, Welfare & Family Affairs, Republic of Korea. (HI14C3417, H18C1178)

This work was supported by the National Research Foundation of Korea (NRF) grant funded by the Korea government (MSIT) (No. 2019R1A2027588)

This work was supported by the National Research Foundation of Korea (NRF) grant funded by the Korea government (MSIT) (No. 2020R1A2C3004123)


### Authors' contributions

Study design: JWK., NRP., and JHJ. Data collection: JWK., NRP., JWK., YNK., HRJ., and JHJ,. Data analysis: JWK., NRP., YNK., HRJ., and JHJ., Data interpretation: JWK., NRP., YNK.,HRJ., and JHJ,. Drafting manuscript: JWK,. and JHJ,. All authors proofread and approved the manuscript.


### Acknowledgements

Not applicable.


# References


1. Armas LA, Recker RR. Pathophysiology of osteoporosis: new mechanistic insights. Endocrinol Metab Clin North Am. 2012;41(3):475–86.
2. Raisz LG. Pathogenesis of osteoporosis: concepts, conflicts, and prospects. J Clin Investig. 2005;115(12):3318–25.
3. Diab DL, Watts NB. Postmenopausal osteoporosis. Curr Opin Endocrinol Diabetes Obes. 2013;20(6):501–9.
4. Ishtiaq S, Fogelman I, Hampson G. Treatment of post-menopausal osteoporosis: beyond bisphosphonates. J Endocrinol Investig. 2015;38(1):13–29.
5. Ha KY, Park KS, Kim SI, Kim YH: **Does bisphosphonate-based anti-osteoporosis medication affect osteoporotic spinal fracture healing?** *Osteoporosis international: a journal established as result of cooperation between the European Foundation for Osteoporosis and the National Osteoporosis Foundation of the USA* 2016, **27**(2):483–488.
6. Anagnostis P, Gkekas NK, Potoupnis M, Kenanidis E, Tsiridis E, Goulis DG. New therapeutic targets for osteoporosis. Maturitas. 2019;120:1–6.

7. Siddiqui JA, Partridge NC. Physiological Bone Remodeling: Systemic Regulation and Growth Factor Involvement. Physiology. 2016;31(3):233–45.
8. de Castro LF, Lozano D, Portal-Nunez S, Maycas M, De la Fuente M, Caeiro JR, Esbrit P. Comparison of the skeletal effects induced by daily administration of PTHrP (1–36) and PTHrP (107–139) to ovariectomized mice. Journal of cellular physiology. 2012;227(4):1752–60.
9. Wang H, Liu J, Yin Y, Wu J, Wang Z, Miao D, Sun W. Recombinant human parathyroid hormone related protein 1–34 and 1–84 and their roles in osteoporosis treatment. PloS one. 2014;9(2):e88237.
10. Khosla S, Hofbauer LC. Osteoporosis treatment: recent developments and ongoing challenges. The lancet Diabetes endocrinology. 2017;5(11):898–907.
11. Kostenuik PJ, Bolon B, Morony S, Daris M, Geng Z, Carter C, Sheng J. Gene therapy with human recombinant osteoprotegerin reverses established osteopenia in ovariectomized mice. Bone. 2004;34(4):656–64.
12. Baltzer AW, Whalen JD, Wooley P, Latterman C, Truchan LM, Robbins PD, Evans CH. Gene therapy for osteoporosis: evaluation in a murine ovariectomy model. Gene therapy. 2001;8(23):1770–6.
13. Bolon B, Carter C, Daris M, Morony S, Capparelli C, Hsieh A, Mao M, Kostenuik P, Dunstan CR, Lacey DL, et al. Adenoviral delivery of osteoprotegerin ameliorates bone resorption in a mouse ovariectomy model of osteoporosis. Molecular therapy: the journal of the American Society of Gene Therapy. 2001;3(2):197–205.
14. Saito H, Gasser A, Bolamperti S, Maeda M, Matthies L, Jahn K, Long CL, Schluter H, Kwiatkowski M, Saini V, et al. TG-interacting factor 1 (Tgif1)-deficiency attenuates bone remodeling and blunts the anabolic response to parathyroid hormone. Nature communications. 2019;10(1):1354.
15. Kay MA, He CY, Chen ZY. A robust system for production of minicircle DNA vectors. Nature biotechnology. 2010;28(12):1287–9.
16. Park N, Rim YA, Jung H, Kim J, Yi H, Kim Y, Jang Y, Jung SM, Lee J, Kwok SK, et al. Etanercept-Synthesising Mesenchymal Stem Cells Efficiently Ameliorate Collagen-Induced Arthritis. Scientific reports. 2017;7:39593.
17. Yi H, Kim Y, Kim J, Jung H, Rim YA, Jung SM, Park SH, Ju JH. A new strategy to deliver synthetic protein drugs: self-reproducible biologics using minicircles. Scientific reports. 2014;4:5961.
18. Rim YA, Yi H, Kim Y, Park N, Jung H, Kim J, Jung SM, Park SH, Ju JH. Self in vivo production of a synthetic biological drug CTLA4Ig using a minicircle vector. Scientific reports. 2014;4:6935.
19. Yasuda T, Banville D, Hendy GN, Goltzman D. Characterization of the human parathyroid hormone-like peptide gene. Functional and evolutionary aspects. J Biol Chem. 1989;264(13):7720–5.
20. Klinck J, Boyd SK. The magnitude and rate of bone loss in ovariectomized mice differs among inbred strains as determined by longitudinal in vivo micro-computed tomography. Calcif Tissue Int. 2008;83(1):70–9.
21. Greenwood C, Clement JG, Dicken AJ, Evans JP, Lyburn ID, Martin RM, Rogers KD, Stone N, Adams G, Zioupos P. The micro-architecture of human cancellous bone from fracture neck of femur patients in

relation to the structural integrity and fracture toughness of the tissue. Bone reports. 2015;3:67–75.

22. Bouxsein ML, Boyd SK, Christiansen BA, Guldberg RE, Jepsen KJ, Muller R. Guidelines for assessment of bone microstructure in rodents using micro-computed tomography. Journal of bone mineral research: the official journal of the American Society for Bone Mineral Research. 2010;25(7):1468–86.
23. Eastell R, Szulc P. Use of bone turnover markers in postmenopausal osteoporosis. The lancet Diabetes endocrinology. 2017;5(11):908–23.

# Figures

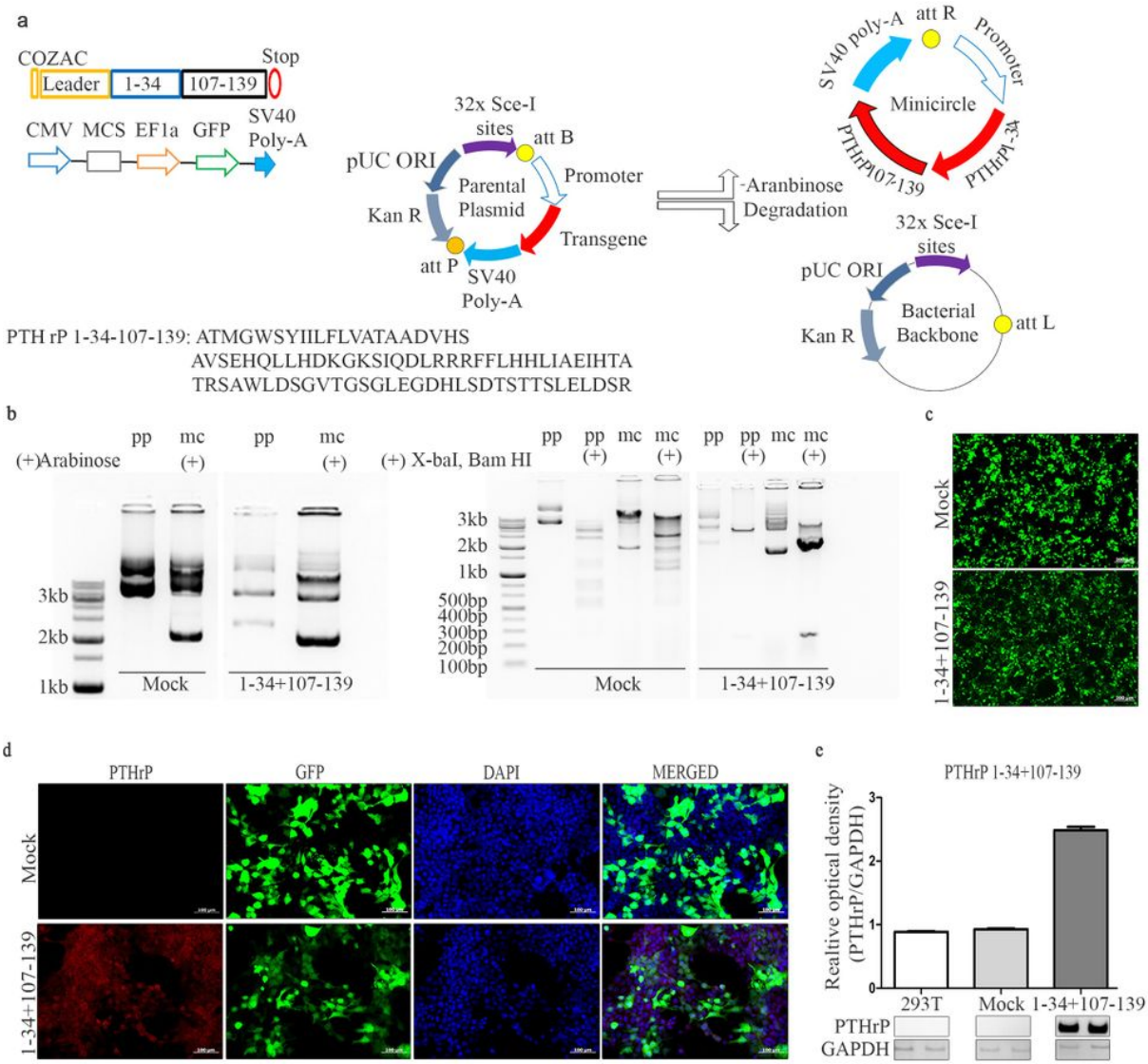

## Figure 1

Production of mc PTHrP 1-34+107-139 vector and transfection in HEK 293T cells. A Clone of PTHrP 1-34+107-139 gene sequence into the parental plasmid; vector map of the parental plasmid, CMV-MCS-EF1a-GFP-SV40PolyA; gene sequence transformation into ZYCY10P3S2T E.Coli cells; DNA vectors are produced from any bacterial plasmid DNA back-bone using arabinose. B The representative parental and minicircle plasmids based on gel images (Mock, and 1-34+107-139). Digestion of Mock, 1-34+107-139 with X-baI and Bam HI confirmed the existence of inserted sequence. C GFP (green) expression of minicircle vector is shown at 48 h post-transfection in HEK 293T cells, at a magnification of x 50; scale bar = 200 μm. D Co-localized immunofluorescence staining of PTHrP (red) with GFP in HEK 293T cells at a magnification of x200; scale bar= 100 μm. E Representative RT-PCR image for the detection of PTHrP 1-34+107-139 gene expression in HEK 293T cell lysate at 48 h post-transfection (293T n = 2, Mock n = 2, 1-34+107-139 n = 2).

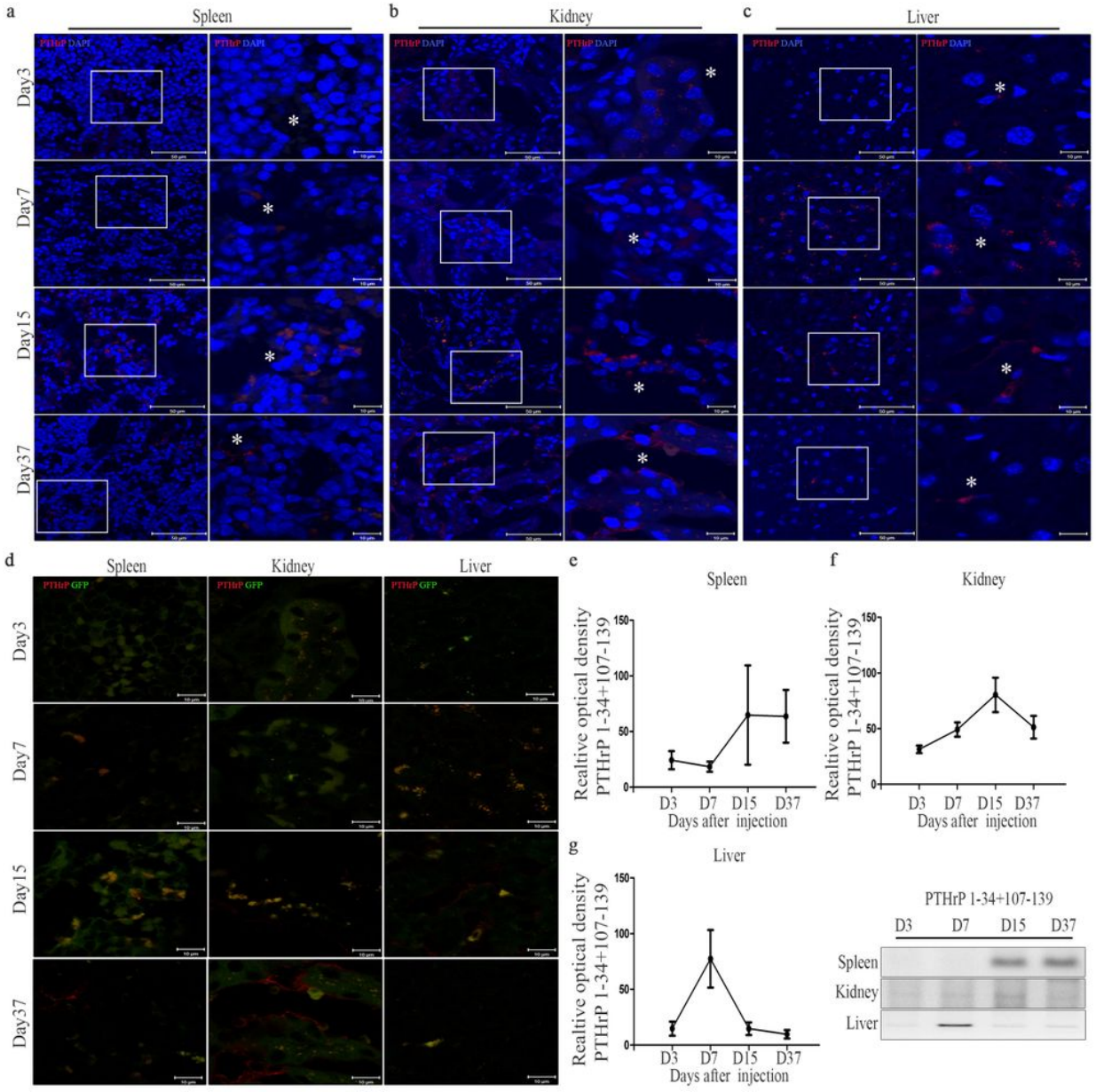


## Figure 2

Life-span of injected mc PTHrP 1-34+107-139 in vivo. A Representative PTHrP expression of mc PTHrP 1-34+107-139 in the spleen of C57BL6 female mice is shown by immunofluorescence staining. At 3, 7, 15, and 37 days after injection, magnification is x 400 and x 1000; scale bar = 50 and 10 μm. B Time-course analysis of PTHrP expression using mc PTHrP 1-34+107-139 in the kidney. C Results of the PTHrP expression in the liver tissue are shown by immunofluorescence staining. D Representative co-staining was performed to observe PTHrP expression of GFP positive cells, magnification is x 1000; 10 μm. E Gene expression of PTHrP 1-34+107-139 in the spleen time-course analysis using RT-PCR. F Gene expression of PTHrP 1-34+107-139 in the kidney time-course analysis using RT-PCR. G Gene expression

of PTHrP 1-34+107-139 in the liver time-course analysis using RT-PCR (n = 2 per time point, immunofluorescence staining and RNA extraction of organ tissues).

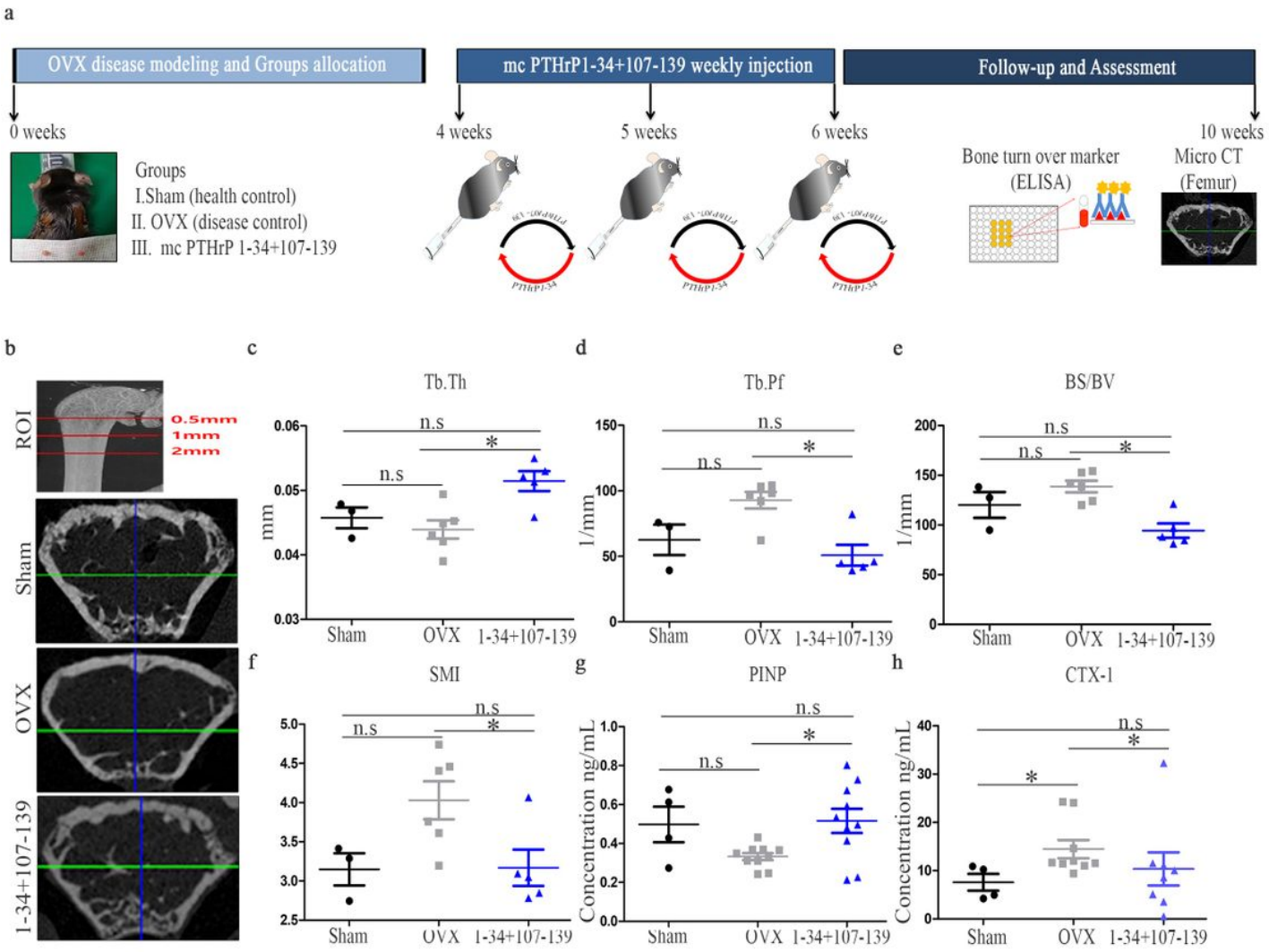


## Figure 3

Assessment of bone quantity and quality using micro CT, and bone formation and resorption in serum at 10 weeks post-OVX. A Schematic diagram of experiments using mc PTHrP 1-34+107-139 injection in an OVX mouse model injected intravenously three times weekly with mc PTHrP 1-34+107-139. B The representative 2D image micro CT of femurs. C-F Assessment of bone quality at 10 weeks post-OVX. C-D Trabecular bone thickness (Tb.Th) and trabecular bone pattern factor (Tb.Pf). E-F The quality of trabecular bone surface (BS/BV) and structural model index (SMI) (sham n = 3, OVX n = 6, 1-34+107-139 n = 5). G PINP was used as a bone formation marker in serum at 10 weeks post-OVX. Mice injected with 1-34+107-139 showed a statistically significant increase in serum bone formation markers compared with mice treated with OVX mice(sham n = 4, OVX n = 10, 1-34+107-139 n = 10 each group). H CTX-1 was used as a serum bone resorption marker at 10 weeks post-OVX. Treatment with 1-34+107-139 resulted in a significantly lower bone resorption compared with the OVX mice (sham n = 4, OVX n = 9, 1-34+107-139 n = 8). Data represent mean ± SEM. Kruskal-Wallis test was used for data analysis and inter-group

comparisons were carried out by Mann-Whitney analysis. * p < 0.05, n.s = not significant. (ROI = Region of Interest, Sham = health control, and OVX = disease control).

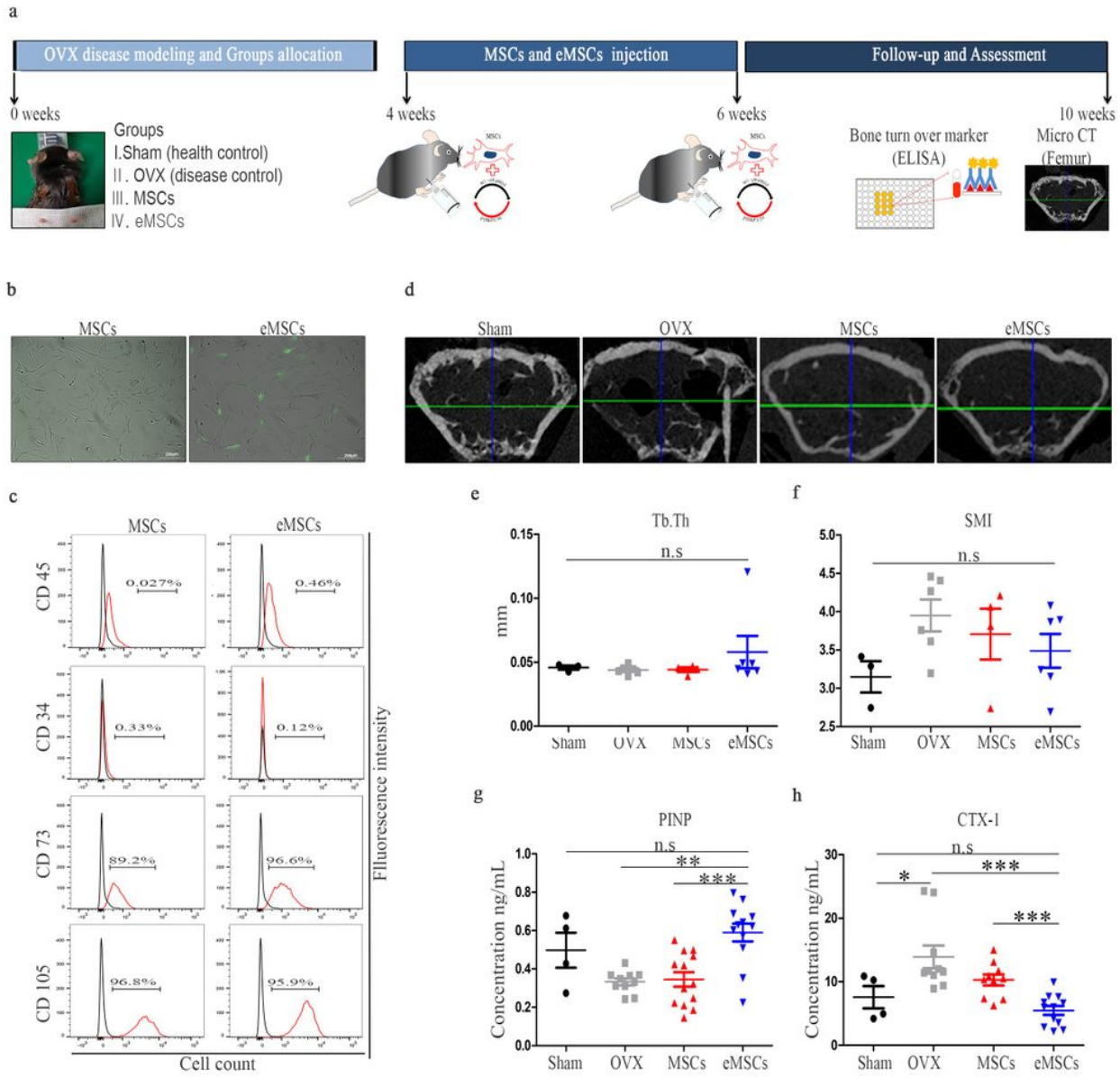


## Figure 4

Therapeutic application of eMSCs injection in OVX mouse model. A Injection of MSCs and eMSCs into an OVX mouse model. MSCs and eMSCs were injected twice (4 and 6 weeks) weekly intraperitoneally (sham n = 3, OVX n = 6, MSCs n = 4, eMSCs n = 6). B Fluorescence images showing the expression of GFP at 48 h after transfection; magnification x 50; scale bar = 200 μm. C Characterization of eMSCs: The percentage of cell expression of each MSC marker was analyzed using CD45 and CD34 as negative markers, and CD73 and CD105 as positive markers. D The representative 2D image micro CT of femurs. E The quality of trabecular bone thickness (Tb.Th). F The quality of trabecular bone structural model index

(SMI). G PINP was used as a bone formation marker in serum at 10 weeks post-OVX (sham n = 4, OVX n = 10, MSCs n = 13, eMSCs n = 12). H CTX-1 was used as a bone resorption marker in the serum at 10 weeks post-OVX (sham n = 4, OVX n = 10, MSCs n = 10, eMSCs n = 12). Data represent mean ± SEM. Kruskal-Wallis test was used for data analysis and inter-group comparisons were performed via Mann-Whitney analysis. * $p < 0.05$, ** $p < 0.01$, ***$p < 0.001$, n.s = not significant. (eMSCs = mc PTHrP1-34+107-139MSCs; sham = health control, OVX=disease control).